

Dynamics of a Rotated Orthogonal Gravitational Wedge Billiard

K. D. Anderson

Abstract

We investigate a rotated, orthogonal gravitational wedge billiard—a special case of the asymmetric gravitational wedge billiard—in which the dynamics are integrable. We derive equations and conditions under which periodic orbits may be constructed for this model, and show that any other trajectory will be dense in the configuration space.

1 Introduction

Based on previous work on the asymmetric wedge billiard [1, 2], we now investigate a special case of the asymmetric wedge billiard which leads to integrable dynamics.

For this special case, we set $\theta_1 = \theta$ and $\theta_2 = \pi/2 - \theta$ in the asymmetric wedge billiard [1, 2]. This corresponds to an orthogonal wedge which is rotated by an angle θ from the vertical, see Figure 1.

This work generalises the work done by Lehtihet and Miller [3], Richter et. al. [4], and Szeredi [5, 6] on the symmetric orthogonal gravitational wedge billiard. For

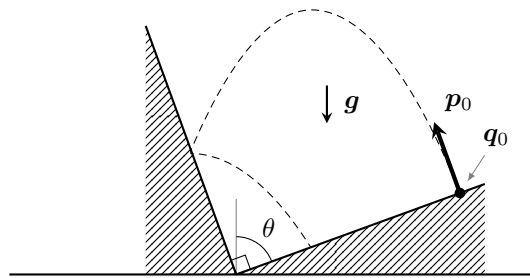


FIGURE 1 The rotated orthogonal wedge billiard.

that specific model, one can show [1] the existence of a period-1 orbit in the billiard, illustrated in Figure 2, which corresponds to fixed-point solutions of the collision maps.

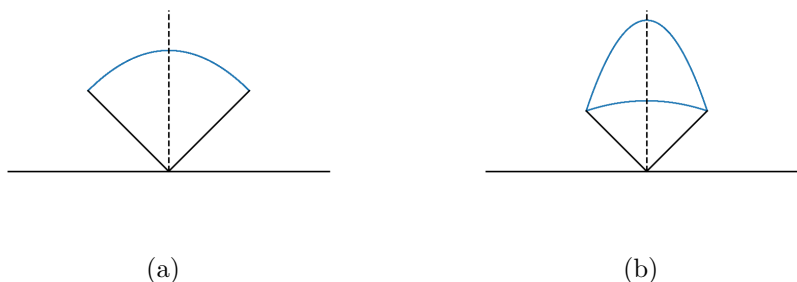


FIGURE 2 Periodic orbits of the symmetric orthogonal gravitational wedge billiard, represented in configuration space (x, y) .

2 Model

2.1 Geometry

We consider the motion of a point particle of mass m within a constant gravitational field \mathbf{g} , its motion restricted to the regions

$$\begin{aligned}\mathcal{Q}_A &= \{(x, y) \in \mathbb{R}^2 : x \geq 0, y \geq x \cot(\theta)\}, \\ \mathcal{Q}_B &= \{(x, y) \in \mathbb{R}^2 : x < 0, y \geq x \tan(\theta)\},\end{aligned}$$

with corresponding boundaries

$$\begin{aligned}\partial\mathcal{Q}_A &= \{(x, y) \in \mathbb{R}^2 : x \geq 0, y = x \cot(\theta)\}, \\ \partial\mathcal{Q}_B &= \{(x, y) \in \mathbb{R}^2 : x \leq 0, y = x \tan(\theta)\},\end{aligned}$$

as illustrated in Figure 3. The real-valued variable θ represents the angle measured clockwise from the vertical and may take values on the interval $(0, \pi/2)$.

We shall call the set $\partial\mathcal{Q} := \partial\mathcal{Q}_A \cup \partial\mathcal{Q}_B$ the *rotated orthogonal wedge*. The boundary $\partial\mathcal{Q}_A$ shall be called the *right-hand slope* or *right-hand wall* of the wedge; similarly, the boundary $\partial\mathcal{Q}_B$ shall be called the *left-hand slope* or *left-hand wall* of

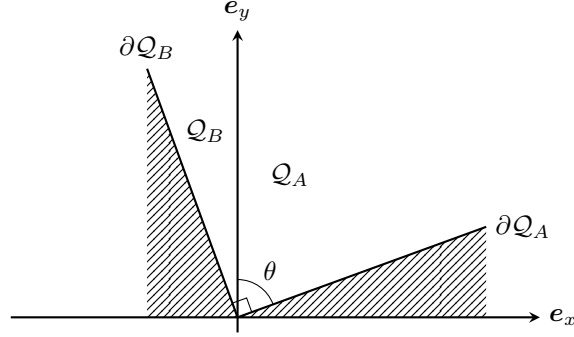


FIGURE 3 Regions of motion and boundaries for the rotated orthogonal wedge billiard.

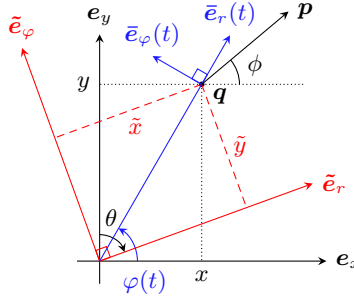


FIGURE 4 Reference systems used in our study of the rotated orthogonal wedge billiard. (Colour online)

the wedge. The intersection of the two boundaries $\partial Q_A \cap \partial Q_B$ shall be called the *wedge vertex*. The region $Q := Q_A \cup Q_B$ is called the *region of allowed motion*.

We introduce an inertial Cartesian reference system such that the origin O is fixed at the wedge vertex, the reference axes with unit vectors $\mathbf{e}_x = [1 \ 0]^T$ and $\mathbf{e}_y = [0 \ 1]^T$ are orthogonal to each other and directed along the horizontal and vertical, respectively, as illustrated in Figure 4. We shall denote by \mathcal{B}_C the set $\{\mathbf{e}_x, \mathbf{e}_y\}$.

Of import in later sections, will be the additional reference systems $\mathcal{B}_R = \{\bar{\mathbf{e}}_r, \bar{\mathbf{e}}_\varphi\}$ with origin coinciding with the particle, and $\mathcal{B}_W = \{\tilde{\mathbf{e}}_r, \tilde{\mathbf{e}}_\theta\}$ with origin coinciding with that of \mathcal{B}_C , as illustrated in Figure 4. The former, introduced by Lehtihet and Miller [3], is dynamic and changes during the motion of the particle; while the latter,

introduced by Szeredi [6], is fixed with its reference vectors coinciding with the wedge walls.

2.2 Mechanics

Let t be the variable representing time and let $\mathbf{q} := \mathbf{q}(t) \in \mathcal{Q}$ represent the position vector at some time t , and let $\mathbf{p} := \mathbf{p}(t) \in \mathbb{R}^2$ represent the momentum vector of the particle at some time t . In the Cartesian reference system, under a transformation to dimensionless quantities [1], we have the coordinate vectors $[\mathbf{g}]_C = [0 \ -1]^T$, $[\mathbf{q}]_C = [x \ y]^T$ and $[\mathbf{p}]_C = [u \ w]^T$. The corresponding Hamiltonian function is

$$H(x, y, u, w) = \frac{u^2 + w^2}{2} + y. \quad (1)$$

Integrating the Hamiltonian equations of motion, derived from the Hamiltonian (1), we find that the particle moves along a parabolic path until it collides with either of the two walls $\partial\mathcal{Q}_j$ ($j = \{A, B\}$). These collisions are assumed to be elastic and obey the reflection law. Since the motion between collisions is completely determined, we focus only on the collision points themselves. The collision maps simplify remarkably in the \mathcal{B}_R reference system. For successive collisions on $\partial\mathcal{Q}_A$, we have the map $F_A : \partial\mathcal{Q}_A \rightarrow \partial\mathcal{Q}_A$ given by

$$\bar{u}_{j+1} = \bar{u}_j - 2\bar{w}_j \cot(\theta), \quad (2a)$$

$$\bar{w}_{j+1}^2 = \bar{w}_j^2. \quad (2b)$$

Similarly, for successive collisions on $\partial\mathcal{Q}_B$, we have the map $G_A : \partial\mathcal{Q}_B \rightarrow \partial\mathcal{Q}_B$ given by

$$\bar{u}_{j+1} = \bar{u}_j + 2\bar{w}_j \tan(\theta), \quad (3a)$$

$$\bar{w}_{j+1}^2 = \bar{w}_j^2. \quad (3b)$$

For a collision with the opposite wall $\partial\mathcal{Q}_B$ for the particle starting on $\partial\mathcal{Q}_A$, we have the map $F_B : \partial\mathcal{Q}_A \rightarrow \partial\mathcal{Q}_B$ given by

$$\bar{u}_{j+1} = \bar{w}_j - (\bar{u}_j + \bar{w}_{j+1}) \tan(\theta), \quad (4a)$$

$$\bar{w}_{j+1}^2 = 2E - \bar{w}_j^2. \quad (4b)$$

Similarly, for a collision with $\partial\mathcal{Q}_A$ for the particle starting on $\partial\mathcal{Q}_B$, we have the map $G_B : \partial\mathcal{Q}_B \rightarrow \partial\mathcal{Q}_A$ given by

$$\bar{u}_{j+1} = -\bar{w}_j - (\bar{u}_j - \bar{w}_{j+1}) \cot(\theta) \quad (5a)$$

$$\bar{w}_{j+1}^2 = 2E - \bar{w}_j^2. \quad (5b)$$

2.3 One-dimensional approximation of motion

We now consider the transformation of the Hamiltonian from the Cartesian reference system \mathcal{B}_C to the reference system \mathcal{B}_W . (The transformations between the different reference systems is detailed in Appendix A.)

Let $\mathbf{q} = [x \ y]^T$ and $\mathbf{p} = [u \ w]^T$ denote the coordinate vectors in \mathcal{B}_C , as previously mentioned. We shall denote the corresponding position and momentum coordinate vectors in \mathcal{B}_W by $\tilde{\mathbf{q}} = [\tilde{x} \ \tilde{y}]^T$ and $\tilde{\mathbf{p}} = [\tilde{u} \ \tilde{w}]^T$.

Rewriting the Hamilton function (1) in terms of the \mathcal{B}_W coordinates yields

$$\tilde{H} = H(\tilde{x}, \tilde{y}, \tilde{u}, \tilde{w}) = \frac{\tilde{u}^2}{2} + \tilde{x} \cos(\theta) + \frac{\tilde{w}^2}{2} + \tilde{y} \sin(\theta). \quad (6)$$

Define

$$\tilde{H}_{\tilde{x}} := \frac{\tilde{u}^2}{2} + \tilde{x} \cos(\theta), \quad \tilde{H}_{\tilde{y}} := \frac{\tilde{w}^2}{2} + \tilde{y} \sin(\theta) \quad (7)$$

and note that both $H_{\tilde{x}}$ and $H_{\tilde{y}}$ are Hamiltonians associated with the one dimensional motion of a particle in a (rotated) gravitational field. Thus, if we suppose that \tilde{y}, \tilde{w} is small enough, which corresponds to particle motion very close to $\partial\mathcal{Q}_A$, then $H_{\tilde{y}} \rightarrow 0$ and $\tilde{H} \approx H_{\tilde{x}}$. A similar argument holds for $H_{\tilde{y}}$ for very small \tilde{x}, \tilde{u} .

The equations of motion for the particle very close to $\partial\mathcal{Q}_A$ are

$$\tilde{x}(t) = t\tilde{u}_0 - \frac{t^2 \cos(\theta)}{2}, \quad (8a)$$

$$\tilde{u}(t) = \tilde{u}_0 - t \cos(\theta) \quad (8b)$$

and for the particle very close to $\partial\mathcal{Q}_B$ are

$$\tilde{y}(t) = t\tilde{w}_0 - \frac{t^2 \sin(\theta)}{2}, \quad (9a)$$

$$\tilde{w}(t) = \tilde{w}_0 - t \sin(\theta). \quad (9b)$$

From the Hamiltonians (7) we may derive bounds on the trajectories in the configuration space:

$$0 \leq \tilde{x}(t) \leq \frac{E}{\cos(\theta)}, \quad 0 \leq \tilde{y}(t) \leq \frac{E}{\sin(\theta)}, \quad (10)$$

where E is the constant energy fixed at the start of the particle's motion.

3 Dynamics

3.1 Fixed points of the collision maps

The maps F_A and G_A have the family of fixed points $(\bar{u}^*, \bar{w}^*) = (c, 0)$ where $c \in \mathbb{R}$ is a constant. This corresponds to the particle sliding up ($c > 0$) or down ($c < 0$) either $\partial\mathcal{Q}_A$ or $\partial\mathcal{Q}_B$

For the maps F_B and G_B , we obtain

$$\bar{u}^* = \sqrt{E} \left(\frac{1 - \tan(\theta)}{1 + \tan(\theta)} \right), \quad \bar{w}^* = \sqrt{E}, \quad (11)$$

and

$$\bar{u}^* = \sqrt{E} \left(\frac{\cot(\theta) - 1}{\cot(\theta) + 1} \right), \quad \bar{w}^* = \sqrt{E}, \quad (12)$$

respectively. In the symmetric wedge billiard, these two fixed points are identical and correspond to a period one trajectory, as illustrated by Figure 2a. To obtain a similar period one trajectory for the rotated orthogonal wedge billiard, we would need to reflect the momentum component across both \bar{e}_r and \bar{e}_φ at the collision point, and set it equal to (11), which results in $[\bar{u}' \ \bar{w}']^T = [-\bar{u} \ -\bar{w}]^T$. However, such a reflection is only possible when $\theta = \pi/4$.

3.2 Periodic orbits

Using equations (8b) and (9b), we may define the following time maps for collisions with the wedge walls in the one-dimensional approximation:

$$t_{j+1}^A = \frac{2\tilde{u}(t_j)}{\cos(\theta)} = 2jT_A, \quad T_A := \frac{\tilde{u}_0}{\cos(\theta)} \quad (13)$$

and

$$t_{k+1}^B = \frac{2\tilde{w}(t_k)}{\sin(\theta)} = 2kT_B, \quad T_B := \frac{\tilde{w}_0}{\sin(\theta)}, \quad (14)$$

with $j, k \in \{0, 1, 2, \dots\}$. The trajectories of the particle's motion will be dense if T_A/T_B is irrational, illustrated in Figure 5. The ratio T_A/T_B is rational for

$$\theta^* = \arctan\left(\frac{p}{q}\right), \quad (15)$$

where $p, q \in \mathbb{N}$ such that $p > 0$, $q > 0$ and $\gcd(p, q) = 1$. To prove this, note that

$$\frac{T_A}{T_B} = \frac{\tilde{u}_0}{\tilde{w}_0} \tan(\theta)$$

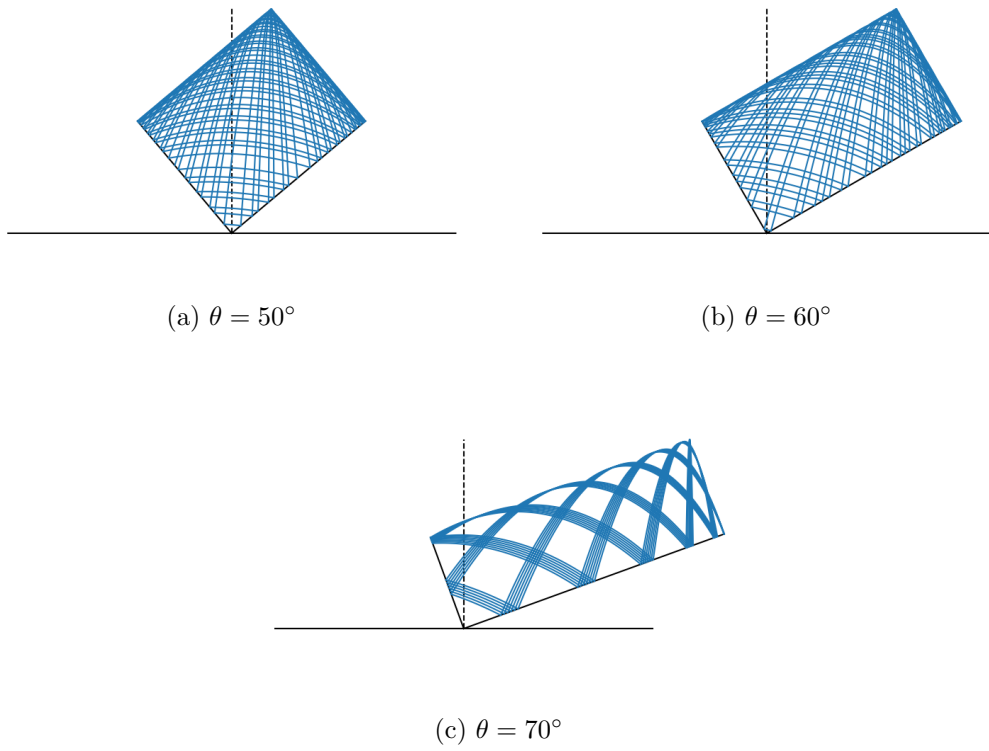


FIGURE 5 Dense trajectories in the rotated orthogonal wedge billiard for various θ , $\phi = 90^\circ$, $\bar{u}_0 = 0$ and $\bar{w}_0 = 1$, after 50 collisions.

which may be simplified to

$$\frac{T_A}{T_B} = \tan(\theta) \quad (16)$$

if we make the substitutions $\tilde{u}_0 = \bar{u}_0$ and $\tilde{w}_0 = \bar{u}_0$ for the particle close to $\partial\mathcal{Q}_A$ and $\partial\mathcal{Q}_B$ respectively. If we substitute θ^* into equation (16), then

$$\frac{T_A}{T_B} = \tan(\theta^*) = \tan\left(\arctan\left(\frac{p}{q}\right)\right) = \frac{p}{q}$$

and $T_A/T_B \in \mathbb{Q}$. The restriction that p and q be positive follows from the restriction on the allowed values for θ , that is, $\theta \in (0, \pi/2)$.

If $p = q$, then $\theta^* = \pi/4$ which corresponds to the symmetric orthogonal wedge billiard. The fixed points of the collision maps (4) and (5) become identically $(\bar{u}_*, \bar{w}_*) = (0, E)$, which correspond to the period-1 orbit in the symmetric orthogonal wedge billiard, as previously mentioned.

For $p \neq q$, we either have $p > q$, from which follows that $p/q > 1$ and $\theta^* > \pi/4$, or $p < q$, from which follows that $p/q < 1$ and $\theta^* < \pi/4$.

Substituting θ^* into the fixed point equations (11) and (12) yields the identical expression

$$\bar{u}^* = \sqrt{E} \left(\frac{q-p}{q+p} \right), \quad \bar{w}^* = \sqrt{E}. \quad (17)$$

For a particle starting on $\partial\mathcal{Q}_A$, using (17) will yield a periodic orbit of period $p+q$ with p collisions on $\partial\mathcal{Q}_A$ and q collisions on $\partial\mathcal{Q}_B$. The number of collisions per side is determined from

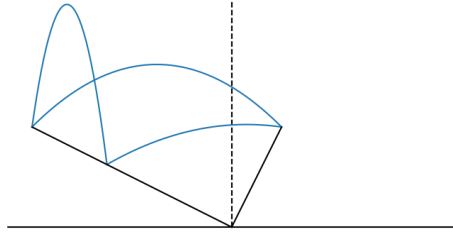
$$\frac{T_A}{T_B} = \frac{p}{q} = \frac{p\bar{u}_0}{\cos(\theta^*)} \frac{\sin(\theta^*)}{q\bar{u}_0} = \frac{p\tilde{u}_0}{\cos(\theta^*)} \frac{\sin(\theta^*)}{q\tilde{w}_0}$$

which leads to

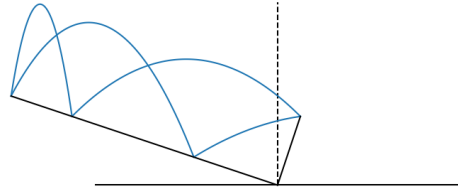
$$t_{p+1}^A = 2pT_A, \quad t_{q+1}^B = 2qT_B$$

in equations (13) and (14). Some examples of periodic orbits are illustrated in Figure 6. Numeric simulations show that these periodic orbits are sensitive with respect to the initial conditions (17)—a small perturbation $\bar{u}^* + \varepsilon$ leads to dense orbits once more.

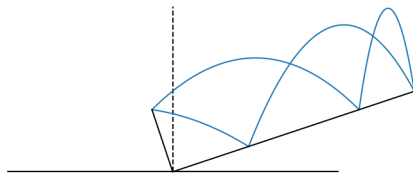
We also plotted the values of θ versus \bar{u} for various p, q in Figure 7. Figure 7a indicate a rotational symmetry in (θ, \bar{u}) space, which allows us to focus on θ -values in $(0, \pi/4]$ generated from suitable p, q values. Of interest are the “windows” which appear for various critical initial θ , we were unable to determine any special relationship between these different θ values with respect each other.



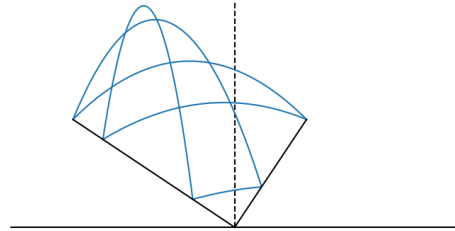
(a) $p = 1, q = 2$



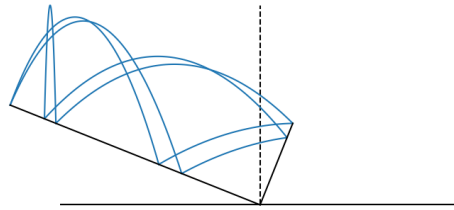
(b) $p = 1, q = 3$



(c) $p = 3, q = 1$

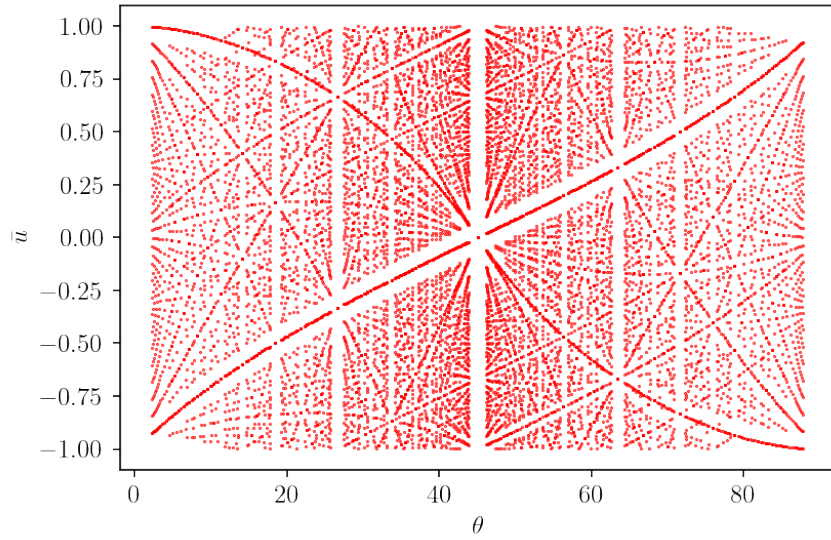


(d) $p = 2, q = 3$

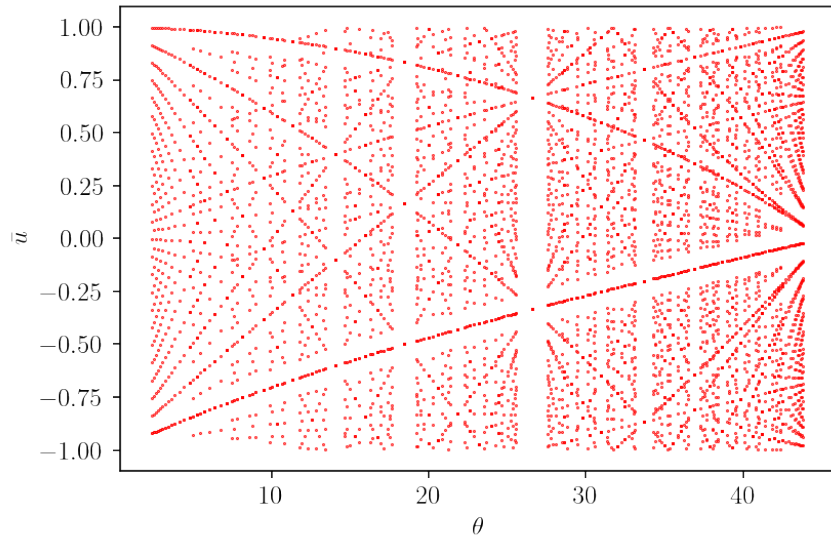


(e) $p = 2, q = 5$

FIGURE 6 Periodic trajectories for a particle launched from $\partial\mathcal{Q}_A$.



(a) $p, q \in \{1, 2, 3, \dots, 25\}$



(b) $p \in \{1, 2, 3, \dots, 25\}, q \in \{p+1, \dots, 25\}$

FIGURE 7 A plot of the \bar{u} component of a periodic trajectory versus θ .

4 Conclusion

We studied a special case of the asymmetric gravitational wedge billiard previously introduced by the author [1, 2]. This extends work on the symmetric orthogonal gravitational wedge billiard previously studied by Lehtihet and Miller [3], Richter et. al. [4], and Szeredi [5, 6].

We derived the conditions under which periodic orbits as well as dense, non-periodic orbits are found. For periodic orbits, we derived an explicit formula for the wedge angle and initial components of the momentum which guarantees a periodic orbit of certain period and known number of collisions on each wall of the wedge. However, numeric simulations show that these periodic orbits are unstable with respect to initial conditions, a small perturbation $\bar{u} + \varepsilon$ leads to dense orbits once more. We were also unable to reproduce Figure 2b using the formula derived for periodic trajectories. The question is whether this is a degenerate case of the orbit presented in Figure 2a or not.

Acknowledgements

This work extends work done in the author's doctoral thesis [1]. The author wishes to thank the University of Johannesburg for the financial assistance and opportunity afforded to pursue the doctorate.

A Coordinate transformations

In this section, we present the technical details of transformations between the various reference systems introduced in section 2.1. Note the time-dependence of the angle φ in Figure 4—this angle changes as the particle moves, whereas θ remains fixed during the motion. Consider the rotation matrix

$$R_\varphi = \begin{bmatrix} \cos(\varphi) & -\sin(\varphi) \\ \sin(\varphi) & \cos(\varphi) \end{bmatrix}$$

and note that

$$\begin{aligned} [\bar{\mathbf{e}}_r \quad \bar{\mathbf{e}}_\varphi] &= [\mathbf{e}_x \quad \mathbf{e}_y] \begin{bmatrix} \cos(\varphi) & -\sin(\varphi) \\ \sin(\varphi) & \cos(\varphi) \end{bmatrix} = [\mathbf{e}_x \quad \mathbf{e}_y] R_\varphi, \\ [\tilde{\mathbf{e}}_r \quad \tilde{\mathbf{e}}_\theta] &= [\mathbf{e}_x \quad \mathbf{e}_y] \begin{bmatrix} \sin(\theta) & -\cos(\theta) \\ \cos(\theta) & \sin(\theta) \end{bmatrix} = [\mathbf{e}_x \quad \mathbf{e}_y] R_{\pi/2-\theta}, \end{aligned}$$

$$[\tilde{\mathbf{e}}_r \quad \tilde{\mathbf{e}}_\theta] = [\bar{\mathbf{e}}_r \quad \bar{\mathbf{e}}_\varphi] \begin{bmatrix} \sin(\theta + \varphi) & -\cos(\theta + \varphi) \\ \cos(\theta + \varphi) & \sin(\theta + \varphi) \end{bmatrix} = [\bar{\mathbf{e}}_r \quad \bar{\mathbf{e}}_\varphi] R_\varphi^T R_{\pi/2-\theta}$$

If we denote the (dimensionless) components of the position and momentum vectors in the different reference systems analogously, that is,

$$\begin{aligned} [\mathbf{q}]_C &= \begin{bmatrix} x \\ y \end{bmatrix}, & [\mathbf{p}]_C &= \begin{bmatrix} u \\ w \end{bmatrix}, & [\mathbf{q}]_R &= \begin{bmatrix} \bar{x} \\ \bar{y} \end{bmatrix}, & [\mathbf{p}]_R &= \begin{bmatrix} \bar{u} \\ \bar{w} \end{bmatrix}, \\ [\mathbf{q}]_W &= \begin{bmatrix} \tilde{x} \\ \tilde{y} \end{bmatrix}, & [\mathbf{p}]_W &= \begin{bmatrix} \tilde{u} \\ \tilde{w} \end{bmatrix}, \end{aligned}$$

then the transformations of the components between the various reference systems are

$$\begin{aligned} [\mathbf{q}]_R &= R_\varphi^T [\mathbf{q}]_C = R_\varphi^T R_{\pi/2-\theta} [\mathbf{q}]_W, & [\mathbf{p}]_R &= R_\varphi^T [\mathbf{p}]_C = R_\varphi^T R_{\pi/2-\theta} [\mathbf{p}]_W, \\ [\mathbf{q}]_W &= R_{\pi/2-\theta}^T [\mathbf{q}]_C = R_{\pi/2-\theta}^T R_\varphi [\mathbf{q}]_R, & [\mathbf{p}]_R &= R_{\pi/2-\theta}^T [\mathbf{p}]_C = R_{\pi/2-\theta}^T R_\varphi [\mathbf{p}]_R. \end{aligned}$$

Also note that

$$[\mathbf{g}]_R = - \begin{bmatrix} \sin(\varphi) \\ \cos(\varphi) \end{bmatrix}, \quad [\mathbf{g}]_W = - \begin{bmatrix} \cos(\theta) \\ \sin(\theta) \end{bmatrix}.$$

For the particle on $\partial\mathcal{Q}_A$, $\varphi = \pi/2 - \theta$ and

$$[\tilde{\mathbf{e}}_r \quad \tilde{\mathbf{e}}_\theta] = [\bar{\mathbf{e}}_r \quad \bar{\mathbf{e}}_\varphi] \begin{bmatrix} 1 & 0 \\ 0 & 1 \end{bmatrix} = [\bar{\mathbf{e}}_r \quad \bar{\mathbf{e}}_\varphi], \quad \begin{bmatrix} \tilde{u} \\ \tilde{w} \end{bmatrix} = \begin{bmatrix} \bar{u} \\ \bar{w} \end{bmatrix}.$$

For the particle on $\partial\mathcal{Q}_B$, $\varphi = \pi - \theta$ and

$$[\tilde{\mathbf{e}}_r \quad \tilde{\mathbf{e}}_\theta] = [\bar{\mathbf{e}}_r \quad \bar{\mathbf{e}}_\varphi] \begin{bmatrix} 0 & 1 \\ -1 & 0 \end{bmatrix} = [-\bar{\mathbf{e}}_\varphi \quad \bar{\mathbf{e}}_r], \quad \begin{bmatrix} \tilde{u} \\ \tilde{w} \end{bmatrix} = \begin{bmatrix} -\bar{w} \\ \bar{u} \end{bmatrix}.$$

References

- [1] K. D. Anderson. *Modelling and computational study of the dynamics of an asymmetric wedge billiard in a constant gravitational field*. PhD thesis, University of Johannesburg, 2019.
- [2] K. D. Anderson and C. M. Villet. Computational study of the dynamics of a gravitational billiard in an asymmetric wedge. *International Journal of Bifurcation and Chaos*, 31(02):2130006, 2021.

- [3] H. Lehtihet and B. Miller. Numerical study of a billiard in a gravitational field. *Physica D: Nonlinear Phenomena*, 21(1):93–104, 1986.
- [4] P. H. Richter, H.-J. Scholz, and A. Wittek. A breathing chaos. *Nonlinearity*, 3(1):45, 1990.
- [5] T. Szeredi. *Classical and quantum chaos in the wedge billiard*. PhD thesis, McMaster University, 1993.
- [6] T. Szeredi. Hard chaos and adiabatic quantization: The wedge billiard. *Journal of Statistical Physics*, 83(1-2):259–274, 1996.